

# Effect of Welding Speed on Fatigue Properties of TC18 Thick Plate by Electron Beam Welding

Han Wen<sup>1,2</sup>, Fu Li<sup>1</sup>, Chen Haiyan<sup>1</sup>

<sup>1</sup> Shaanxi Key Laboratory of Friction Welding Technologies, State Key Laboratory of Solidification Processing, Northwestern Polytechnical University, Xi'an 710072, China; <sup>2</sup> The First Aircraft Institute, Xi'an 710089, China

**Abstract:** The welding of 15 mm thick TC18 titanium alloy thick plate was realized by electron beam welding. The effect of different welding speeds (10, 20, 30 mm/s) on the fatigue properties of the electron beam welded joints for TC18 titanium alloy was investigated. The macroscopic morphology, microstructure and fracture characteristics of the joints were analyzed by optical microscope, scanning electron microscopy and transmission electron microscopy, and the fatigue properties of welded joints were studied and tested by an electronic universal testing machine. The results show that the weld fusion zone is mainly composed of columnar  $\beta$  phase and acicular  $\alpha$  martensite phase. The upper melting width, the middle melting width and the lower melting width are obviously reduced, and the grain size gradually decreases with the increase of welding speed, which results in the increase of fatigue properties of welded joints. At  $N_f=10^7$ , the fatigue limit of the weld increases by nearly 29% with the welding speed from 10 mm/s to 30 mm/s. The fatigue fracture of the joints can be divided into three typical regions of fatigue crack source zone, expansion zone and instantaneous zone, and the fatigue cracks all originate from the surface of the specimen. With the increase of welding speed, the proportion of instantaneous area decreases and the fatigue performance increases.

**Key words:** welding speed; electron beam welding; S-N curve; fatigue performance

TC18 titanium alloy is a kind of high strength, high toughness, weldable near-beta titanium alloy with both the properties of  $\alpha+\beta$  titanium alloy and  $\beta$  titanium alloy<sup>[1]</sup>. The annealing strength is more than 1080 MPa, which is the highest strength of the current annealed titanium alloy, mainly for the manufacture of various large forgings and high bearing capacity of the aviation structure. The prominent advantage of TC18 titanium alloy is that the thickness of harden-through section in air medium can reach 250 mm. Using TC18 titanium alloy instead of traditional high-strength steel can reduce the weight of aircraft structure by about 15%, which is obvious in manufacturing large-scale bearing structure of aircraft advantage<sup>[2-5]</sup>. As an important method of manufacturing aeronautical structure, welding has been studied extensively all over the world. Titanium has strong chemical activity. With the increase of temperature, its chemical activity will also increase rapidly, and it can absorb

all kinds of gases, such as oxygen, nitrogen, hydrogen under solid state<sup>[6]</sup>. While these interstitial elements increase the strength, they reduce ductility and toughness and cause severe embrittlement<sup>[7,8]</sup>. To overcome these problems, electron beam welding (EBW) is considered to be an ideal process to join titanium and its alloys. Electron beam welding has the characteristics of heat concentration, large welding width, high welding speed, good physical properties of joints, small welding residual stress and deformation advantages, easy to achieve high-precision welding, so titanium welding is often used in one of the methods<sup>[9]</sup>. The previous research on TC18 titanium alloy electron beam welding was mainly related to the comparison of heat treatment and the microstructure and properties of different welding methods. There was little research on the influence of the process parameters on the fatigue performance of the weld, especially the effect on the TC18 titanium alloy thick plate. For example, Guo<sup>[10]</sup> et al.

Received date: April 02, 2018

Foundation item: Key Areas of Innovation Team in Shaanxi Province (2014KCT-12)

Corresponding author: Fu Li, Ph. D., Professor, Shaanxi Key Laboratory of Friction Welding Technologies, State Key Laboratory of Solidification Processing, Northwestern Polytechnical University, Xi'an 710072, P. R. China, Tel: 0086-29-88460250, E-mail: fuli@nwpu.edu.cn

Copyright © 2018, Northwest Institute for Nonferrous Metal Research. Published by Elsevier BV. All rights reserved.

measured the tensile and impact properties of welded joints and 4 kinds of post weld heat treatment joints at room temperature. The microstructure and impact fracture of different heat treatment states were observed by optical and scanning electron microscope. The results show that different forms of intragranular  $\alpha$  can be obtained by different heat treatment of TC18 electron beam welds. Guan<sup>[11]</sup> et al. compared and analyzed the mechanical properties of TC18 Ti alloy argon arc welding joint and electron beam welding joint. The results showed that the electron beam welding joint has higher tensile strength and better high cycle fatigue performance, which is more beneficial to engineering applications. Yuan et al. carried out thermal simulation tests on TC18 titanium alloy successively, including manual TIG welding<sup>[12]</sup>, electron beam welding<sup>[13]</sup> and flash butt welding<sup>[14]</sup>. The microstructure and properties of joints under various processes were analyzed. Song<sup>[15]</sup> et al. studied the deformation of electron beam welding of 60 mm TC18 titanium alloy thick plate. The results showed that the electron beam welding of TC18 titanium alloy has little deformation. Hu<sup>[16]</sup> et al. researched TC18 titanium alloy welding to ensure the strength of its welded joint for the first time in the landing gear manufacturing during the development of a certain type of aircraft, including optimal welding parameters and welding joint of TC18 titanium alloy by heat treatment. TC18 titanium alloy is mainly used to manufacture all kinds of high-load bearing aviation components, and the fatigue performance is one of the important assessment indicators. However, the research on the fatigue properties of titanium alloy welded joints and its influencing factors are rarely reported, especially the systematic study on the fatigue properties of TC18 thick welded joints. Based on this, this paper aims to study the influence of welding speed on the fatigue performance of the joint based on 15 mm TC18 thick sheet electron beam welding, and analyze its fracture morphology.

## 1 Experiment

The as-annealed TC18 titanium alloy forgings (chemical composition shown in Table 1) were machined by wire cutting into the size of 100 mm×75 mm×15 mm of the workpiece and welded along the 100 mm×15 mm facing the welding. Before welding, the test piece was cleaned, and the surface of the test plate was polished with a wire brush. The oxide film was removed, and then the surface of the area was wiped to be welded with a silk cloth dipped in ethanol to remove oil stains and foreign debris. The welding experiment was carried out on the KS150-G150 electron beam welding machine. The specific welding parameters used in the experiment were as follows: voltage 150 kV, electron beam 23 mA and focusing current 2090 mA. After welding, the fatigue test specimens were intercepted in three layers, top, middle and bottom, perpendicular to the direction of weld (as shown in Fig.1).

**Table 1 Chemical composition of TC18 (wt%)**

Al	Mo	V	Cr	Fe	Ti
4.4~5.7	4.0~5.5	4.0~5.5	0.5~1.5	0.5~1.5	Bal.

The effect of welding speeds (10, 20, 30 mm/s) on microstructure and fatigue performance of electron beam welded (EBW) joints of TC18 titanium alloy was investigated using the middle layer under the fatigue test conditions: frequency  $f=15$  Hz, cyclic stress ratio  $R=0.5$ , cycle life setting  $N_f=10^7$ .

After welding, the sheets were cut by wire cutting. The welded samples were ground, polished and etched. After being etched with Keller reagent (2 mL hydrofluoric acid, 8 mL nitric acid and 90 mL distilled water), metallographic microscope (OM), scanning electron microscope (SEM) and transmission electron microscopy (TEM) were used to observe the microstructure. The fracture surface was observed by SEM.

## 2 Results and Discussion

In the electron beam welding process, the welding parameters affect the size of the line energy, while the line energy directly determines the heat input of the weld, and further affects the performance of the welded joint. The relationship between the line energy of the electron beam welding and the welding process parameters is as follows:

$$q = \frac{UI}{v} \quad (1)$$

in the formula,  $q$  is the line energy (J/mm),  $U$  is the accelerating voltage (kV),  $I$  is the electron beam current (mA) and  $v$  is the welding speed (mm/s). From Eq. (1), the line energy is determined by the acceleration voltage  $U$ , welding speed  $v$ , electron beam  $I$  and other parameters. In this experiment, the influence of welding speed  $v$  on the performance of welded joints was studied under the condition of keeping  $U$  and  $I$  constant.

### 2.1 Microstructure

The cross-sectional morphology of TC18 electron beam welded joints at different welding speeds are shown in Fig.2. It can be seen that when the welding speed is 10 mm/s, the

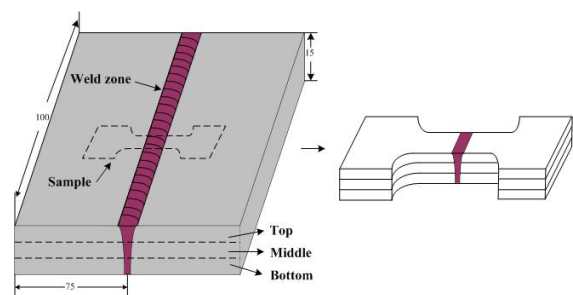


Fig.1 Electron beam welding and sampling diagram of TC18 thick plate

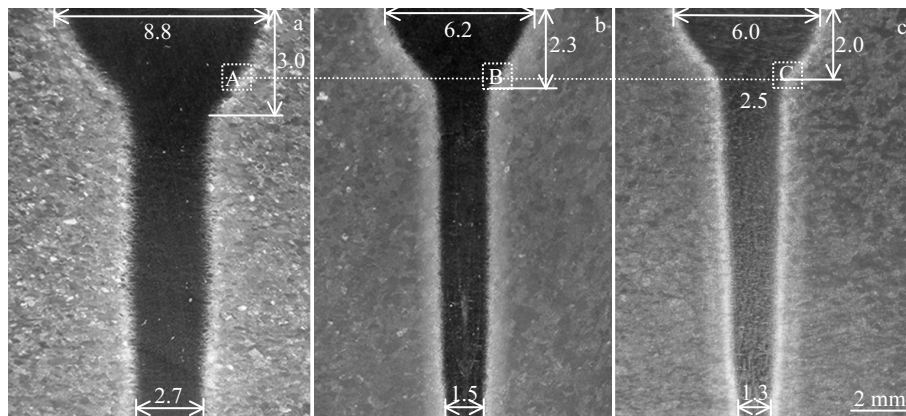


Fig.2 Cross-sectional morphologies of TC18 electron beam welded joints at different welding speeds: (a) 10 mm/s, (b) 20 mm/s, and (c) 30 mm/s

weld appears as a bell-type. As the welding speed increases, it changes into a funnel shape, and the upper part of the funnel, the funnel height and the bottom of the funnel are gradually reduced. This is because when other parameters are constant, the higher welding speed leads to a reduction in the heat input, and at the same time, the high temperature dwell time is reduced, so that the appearance of the weld becomes narrower and closer to the funnel. Fig.3 shows the microstructure of TC18 electron beam welded joints at different welding speeds. It can be seen that the fusion zone (FZ) is mainly composed of fine martensitic  $\alpha$  phase and large grains of  $\beta$  phase owing to the fast cooling during EBW. Due to the high concentration of energy in the electron beam welding process, the central temperature of the weld pool can reach 1800~2300 °C, the residence time of high temperature is relatively short, and the cooling speed is fast. Under the influence of high temperature gradient, the columnar crystals first nucleate at the solid-liquid interface and then grow preferentially to the fastest heat dissipation direction. The center of the weld is the final solidification zone due to the highest temperature and the poor heat dissipation condition, so that the  $\beta$  grain boundary is retained during solidification. In the columnar crystal growth zone, the transition temperature of  $\beta$  phase is lower than that it needs to the transition into  $\alpha$  balanced phase through diffusion

in the rapid solidification and cooling process; as a result, phase transformation occurs only through the  $\beta$ -phase atom migration to form  $\alpha$ -stable element supersaturated solid solution; therefore, columnar crystalline intramural fine needle-like martensite  $\alpha$  phase can be obtained. Edwards et al<sup>[17]</sup> and Akhoni<sup>[18]</sup> also observed the fine acicular microstructure in the FZ of EBW titanium alloy joints. When the welding speed is 10 mm/s, the area of the heat affected zone (HAZ) of the joint is wider, the microstructure is larger, and the size of the columnar grain formed by the FZ is larger. With the increase of welding speed, the heat input decreases, the HAZ width of the joint decreases, the grain size becomes smaller, the size of FZ columnar grain decreases, and the intracellular dendrites are denser. At the welding speed of 30 mm/s, the HAZ has the narrowest width and the smallest grain size, and the cellular dendrites in FZ crystal are the most compact. Therefore, increasing the welding speed can achieve the purpose of refining grain. Fig.4 shows the TEM results of the weld zone at different welding speeds. It can be seen that EBW causes the weld zone to mainly consist of columnar  $\beta$  grains and acicular  $\alpha$ -martensite grains. With the increase of the welding speed, the columnar  $\beta$ -grains and the acicular  $\alpha$ - martensite grains in the weld area become smaller, which is consistent with Fig.3.

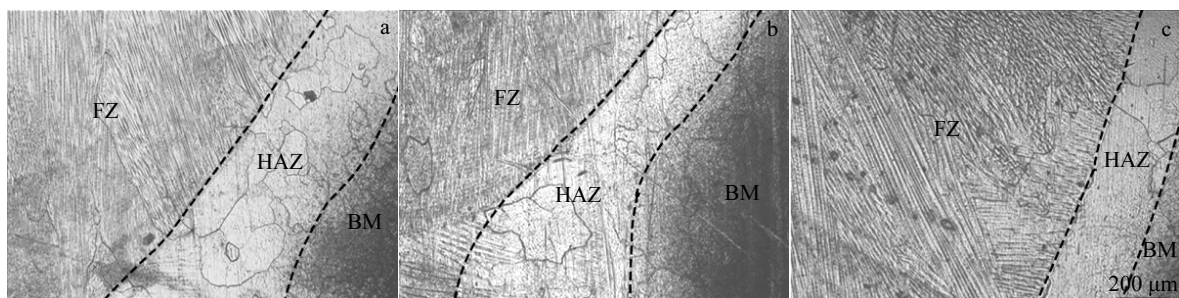


Fig.3 Microstructures of the magnified A (a), B (b) and C (c) points in Fig.2

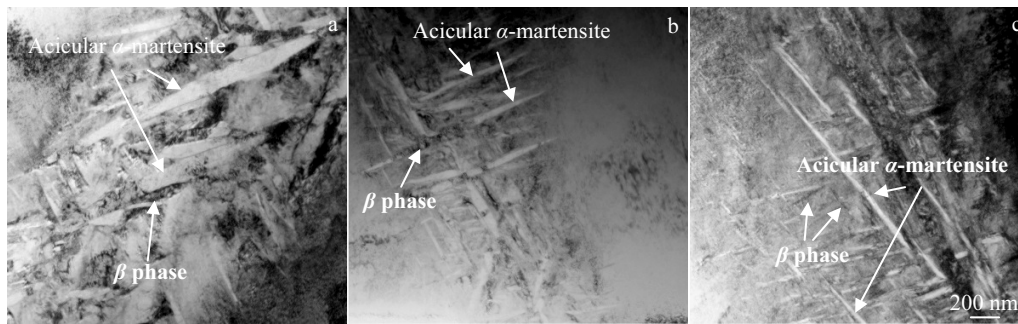


Fig.4 TEM images of TC18 electron beam welded joint zone at different welding speeds: (a) 10 mm/s, (b) 20 mm/s, and (c) 30 mm/s

## 2.2 Fatigue properties

The  $S-N$  curve of welded joints can be expressed as the relationship between fatigue stress  $S$  and fatigue life cycle  $N$  under different cyclic stresses. The most commonly used form of describing material  $S-N$  curves is the power function form, that is:

$$S^m N = C \quad (2)$$

In the formula,  $m$  and  $C$  are the parameters related to material properties, sample form, stress ratio and loading method. Taking the stress  $S$  as a function and the cycle life  $N$  as the independent variable, the test data set ( $N, S$ ) is processed according to the usual standard power function expression. We will get the following formula:

$$S = CN^{\frac{1}{m}} \quad (3)$$

Fitting formula (3), we can get  $S-N$  curve of welded joints at different welding speeds as shown in Fig.5 and  $S-N$  curves of welded joints along the thickness of the plate at the welding speed of 30 mm/s is shown in Fig.6.

It can be seen from Fig.5, as the welding speed increases, the fatigue performance of the welded joints increases, because the weld zone and heat affected zone width become narrower, and the grain size becomes smaller. The stretch deformation, the grain boundary resistance to deformation of the material become larger, increasing anti-fatigue ability, and increasing fatigue limit. Fig.6 shows the  $S-N$  curves along the

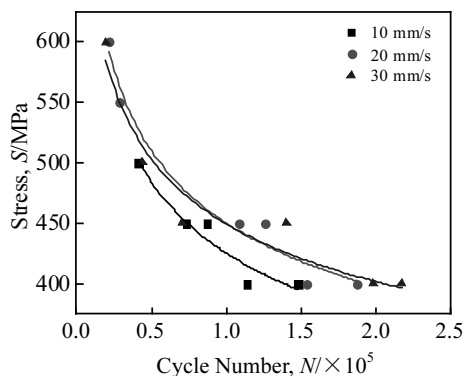


Fig.5  $S-N$  curves of specimens at different welding speeds

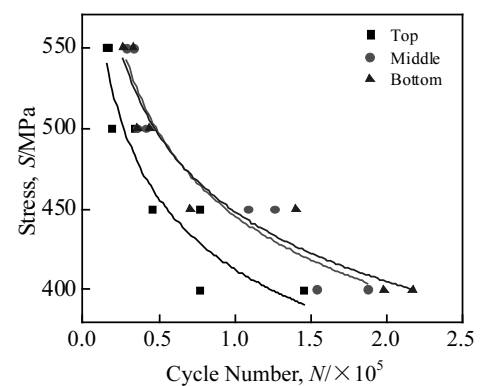


Fig.6  $S-N$  curves of specimens along the thickness of the plate at the welding speed of 30 mm/s

direction of thickness in the three layers of welded joint sections. It can be seen that the fatigue performance of the welded joints from the top to the bottom along the thickness direction gradually increases, because from the top to the bottom of the weld zone, the grain size decreases. Grain refinement not only prevents fatigue cracks from sprouting at grain boundaries, fatigue crack growth, but also improves the ability of joints to resist sliding deformation, suppresses the formation and cracking of cyclic slip bands, thus effectively improving its fatigue performance. According to the fitting curves, the parameters  $C$  and  $n$  of the  $S-N$  curve and the fatigue limit at  $N_f = 10^7$  for the weld of TC18 electron beam welded joint at different welding speeds were obtained, as shown in Table 2. It can be seen that as the welding speed increases, the fatigue strength of the weld gradually increases, and the fatigue limit of the weld increases by nearly 29% with the welding speed from 10 mm/s to 30 mm/s. That is consistent with the results in Fig.5.

## 2.3 Fractography

Fig.7 shows the fatigue fracture morphologies of the joints at different welding speeds. It can be seen that the fatigue cracks originate from the edge of the specimen surface. Most of the specimens show single source characteristics and

**Table 2 Parameters of S-N curve and fatigue strength**

Welding speed, $v/\text{mm}\cdot\text{s}^{-1}$	$C$	$n$	Fatigue strength, $S/\text{MPa}$
10	3638	-0.19	170
20	3551	-0.18	195
30	2907	-0.16	220

extend from one side of the specimen to the other. Due to the samples preparation, the processing of titanium alloy specimen surface inevitably makes processing marks appear, causing stress concentration, as a source of cracks. Since the sample surfaces are in plane stress state, the plastic slip surface cracks more easily than grain slip, so fatigue crack often originates from fatigue specimen surface<sup>[19]</sup>. Fig.7d~7f are fatigue strips. The fatigue strip is the most typical characteristic of fatigue fracture. The fatigue striations and fatigue crack perpendicular to the propagation direction of parallel fatigue striations slightly bend into an arc shape, and the arc center points to the fatigue source region. A fatigue stripe forms at each load cycle, and the distance between the fatigue striations becomes larger with the crack propagation. Fig.7g~7i are the dimple morphologies of the transient zones. It can be seen that the morphologies of the transient zones are

characterized by cracking along the phase boundary and the shape of the last torn dimple. The dimples form when the normal stress is pulled off, and the tear edges are not high. The fracture mechanism of weld joints is the quasi cleavage, and their plasticity B undistinguished.

During the fatigue test, when the crack is enlarged so that the residual cross-section of the object is not enough to resist the external load, and the object suddenly breaks under a certain load. Therefore, the performance of the joint can be compared on the whole fracture ratio in different fatigue fracture zones under the same stress. Fig.7 shows the fatigue fracture morphologies of the welded joints at different welding speeds at the stress 450 MPa. It can be seen that with the increase of welding speed, the proportion of instantaneous break area decreases, which indicates that the fatigue performance of welded joints increases with the increases of welding speed under the condition of accelerating voltage 150 kV. This is because the welding speed is strengthened, the heat input decreases, the grain size decreases, the area of the unit volume grain boundary increases, and the hindrance to deformation becomes stronger, resulting in smaller area of the transient zone, which can resist large pulling force and improve the performance.

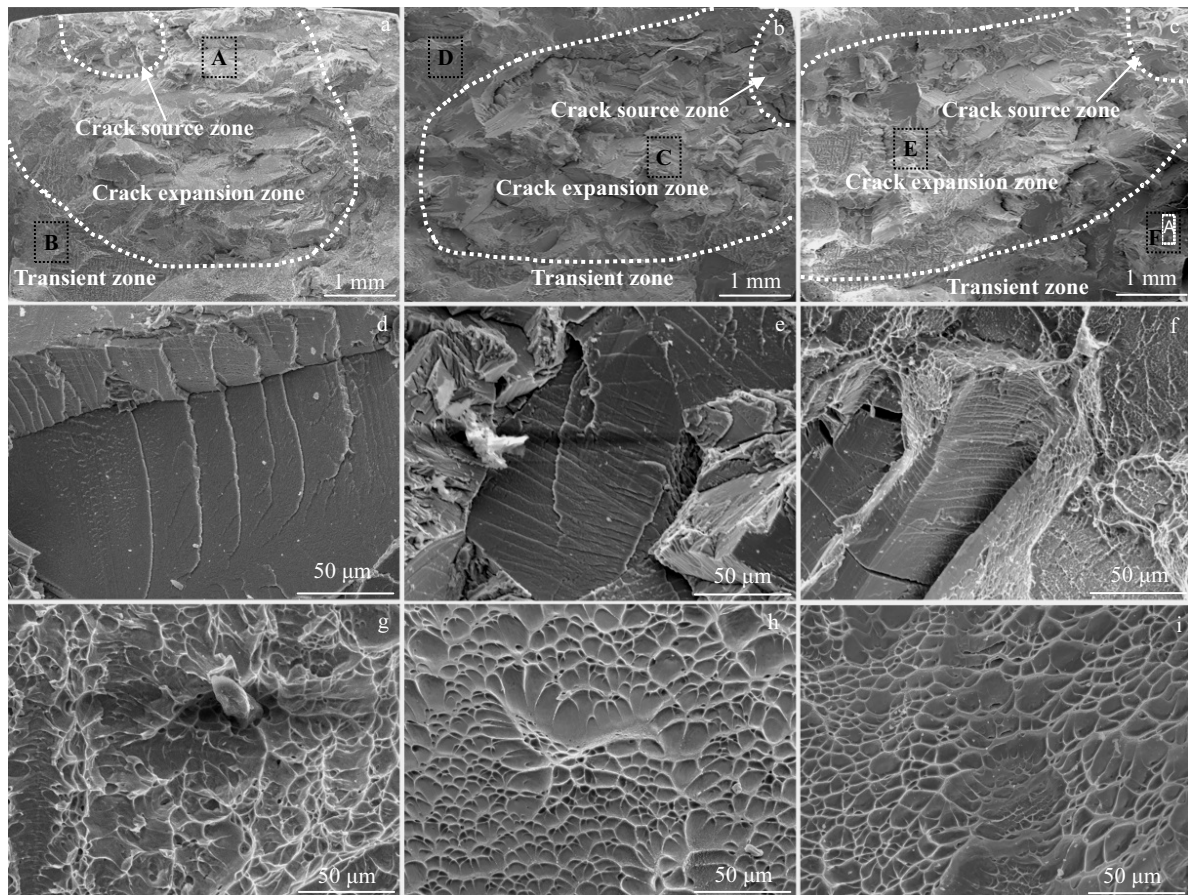


Fig.7 Fatigue fracture morphologies of the joints at different welding speeds: (a) 10 mm/s, (b) 20 mm/s, and (c) 30 mm/s; magnified morphologies of A (d) and B (e) in Fig.7a, C (f) and D (g) in Fig.7b, and E (h) and F (i) in Fig.7c

### 3 Conclusions

1) Under the condition of accelerating voltage 150 kV, focusing current 2090 mA and electron beam 23 mA, through adjusting the welding speed, 15 mm thick TC18 titanium alloy thick plate welding was achieved by electron beam welding. When the welding speed is 30 mm/s, the obtained welded joint has the best performance.

2) The weld fusion zone is mainly composed of columnar  $\beta$  phase and acicular  $\alpha$  martensite phase. With the increase of the welding speed, the grain size of the weld zone becomes smaller and the intragranular dendrite is denser. Under the condition of the welding speed of 30 mm/s, the grain size is the smallest, and the grains are refined.

3) With the increase of the welding speed, the fatigue performance increases. At  $N_f=10^7$ , the fatigue limit of the weld increases by nearly 29% with the welding speed from 10 mm/s to 30 mm/s. The fatigue performance of the welded joint is enhanced along the thickness of the plate at the welding speed of 30 mm/s.

4) The fatigue fracture of the joint can be divided into three typical regions: crack source zone, crack expansion zone and transient zone. The cracks originate at the edge of the specimen surface. The fatigue fracture transient zone is the smallest when the welding speed is 30 mm/s and the fatigue performance is the strongest.

### References

- Zhu Feng, Ji Bo, Zhu Yifan. *Rare Metal Materials and Engineering*[J], 2005, 34(S3): 314
- Wu Aiping, Zhao Haiyan, Shi Qingyu et al. *Aeronautical Manufacturing Technology*[J], 2008(24): 26 (in Chinese)
- Li Jun, Yang Janguo, Weng Lulu et al. *Welding & Joining*[J], 2008(8): 16 (in Chinese)
- Zhang Yong, Yang Jianyuo, Liu Xuesong et al. *Transactions of the China Welding Institution*[J], 2010,19(4): 74 (in Chinese)
- Li Jun, Yang Janguo, Li Hailong et al. *Frontiers of Materials Science in China*[J], 2009, 3(1): 84
- Welsch G, Boyer R, Collings E W. *Materials Properties Handbook: Titanium Alloys*[M]. USA: ASM International, 1994: 829
- Saresh N, Pillai M G, Mathew J. *Journal of Materials Processing Technology*[J], 2007, 192-193: 83
- Barreda J L, Santamaria F, Azpiroz X et al. *Vacuum*[J], 2001, 62(2-3): 143
- Li A B, Huang L J, Meng Q Y et al. *Materials and Design*[J], 2009, 30: 1625
- Guo Shaoqing, Gu Weihua, Yu Huai et al. *Journal of Aeronautical Materials*[J], 2006, 26(3): 116
- Guan D, Sun Q. *Advances in Aeronautical Science and Engineering*[J], 2012, 3(2): 174
- Wang Jinxue, Yuan Hong, Yu Huai et al. *Aerospace Manufacturing Technology*[J], 2008(3): 19 (in Chinese)
- Wang Jinxue, Yuan Hong, Yu Huai. *Welding & Joining*[J], 2010(3): 33 (in Chinese)
- Wang Jinxue, Yuan Hong, Yu Huai et al. *Aerospace Manufacturing Technology*[J], 2013(3): 22 (in Chinese)
- Song Yunfei, Liu Xi, Chang Ming. *The Eighteenth National Symposium on Welding of the Society of Welding of the China Society of Mechanical Engineering, S02 High Energy Beam and Special Welding*[C]. Nanchang: The Chinese Engineering Society, 2013: 188
- Hu Yugang, Wang Xiaoping, Zhou Liang. *Aeronautical Manufacturing Technology*[J], 2011(16): 72 (in Chinese)
- Edwards P D, Ramulu M. *Science and Technology of Welding and Joining*[J], 2009, 14(5): 476
- Akhonin S V, Mishchenko R N, Petrichenko I K. *Materials Science*[J], 2006, 42(3): 323
- Chen Chuanrao. *Fatigue and Fracture*[M]. Wuhan: Huazhong University of Science and Technology Press, 2002: 7 (in Chinese)

## 焊接速度对 TC18 钛合金厚板电子束焊接接头疲劳性能的影响

韩文<sup>1,2</sup>, 傅莉<sup>1</sup>, 陈海燕<sup>1</sup>

(1. 西北工业大学 凝固技术国家重点实验室 陕西省摩擦焊接重点实验室, 陕西 西安 710072)

(2. 中航工业第一飞机设计研究院, 陕西 西安 710089)

**摘要:** 采用电子束焊接的方法, 实现了 15 mm TC18 钛合金厚板的焊接。利用光学显微镜、扫描电镜及透射电子显微镜对接头的宏观形貌、显微组织及断口特征进行分析, 并用电子万能试验机测试了接头的疲劳性能, 研究了不同焊接速度 (10、20、30 mm/s) 对 TC18 钛合金厚板电子束焊接接头疲劳性能的影响。结果表明, 焊缝熔合区主要由柱状的  $\beta$  相和针状的  $\alpha$  马氏体相组成。随着焊接速度的增加, 焊缝区上熔宽、中熔宽、下熔宽都呈明显减少, 焊缝区晶粒细化, 导致焊接接头疲劳性能增加。在  $N_f=10^7$  时, 随焊接速度从 10 mm/s 增加到 30 mm/s, 焊缝疲劳极限提高近 29%。接头疲劳试验断口可分为疲劳裂纹源区、裂纹扩展区和裂纹瞬断区 3 个典型区域, 疲劳裂纹都起源于试件表面, 随着焊接速度增大, 瞬断区占的比例减小, 疲劳性能增强。

**关键词:** 焊接速度; 电子束焊接; S-N 曲线; 疲劳性能